Chapter VI

OPTICAL MICROSCOPY, DSC, SPONTANEOUS POLARIZATION AND FREQUENCY DOMAIN DIELECTRIC SPECTROSCOPY STUDIES ON A FERROELECTRIC LIQUID CRYSTAL

Part of this work was presented at the 20th International Liquid Crystals Conference, Ljubljana, Slovenia, July 2004.

Introduction

Meyer in 1974 [1] concluded from symmetry argument that chiral molecules in smectic C phase should exhibit ferroelectricity and such phenomenon was indeed discovered soon in a Schiff's base DOBAMBC [2], thus started a new branch of material science and technology to study these intrinsic fluid ferroelectric materials. Since the discovery of antiferroelectricity by Fukuda group [3] in MHPOBC it has been shown that between antiferro-, ferro- and para-electric phases three different *subphases* also exist [3-6] and their stability depends strongly on the optical purity of the compounds [7]. Ferroelectric liquid crystals (FLCs) have also been subject of intense investigation for their application in fast switching flat panel displays or optical light modulators [8-10].

Dielectric spectroscopy studies on ferroelectric liquid crystals are important since one can get information about the relaxation modes directly associated with ferroelectricity [11]. The Goldstone mode appears in the SmC^* phase because of the phase fluctuations in the azimuthal orientation of the molecular director (depicted in **Figure 2.13**, Chapter II) and its characteristic frequency is usually less than 10 kHz. The soft mode, on the other hand, appears in the neighbourhood of SmA^*- SmC^* transition due to fluctuations in the tilt angles of the molecules. Although hard to excite in comparison to the Goldstone mode, it softens near the transition point and this mechanism is usually observed at high frequencies. Both these modes are called collective mode since they represent collective behaviour of the molecules under the influence of an ac field. Optical microscopy and DSC study as well as studies on the temperature dependence of spontaneous polarization (which is often considered as the secondary order parameter for the ferroelectric phase [10]) have also been carried out.

In this chapter results of frequency domain dielectric spectroscopy study on a partially fluorinated MHPOBC compound [**MHPO(13F)BC**] has been presented. Lagerwall *et al.* [6] while studying the prototype antiferroelectric liquid

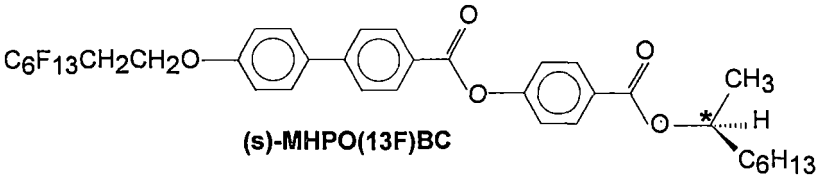

(s)-MHPO(13F)BC

	Cr1	Cr2	SmC*	SmA*	I
ΔH (kCal/mol)	80.7	98.9	149.0	184.0	
	3.02	4.6	0.2	1.13	

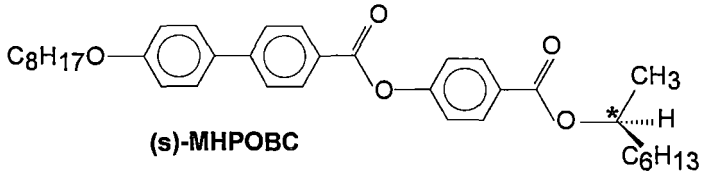

(s)-MHPOBC

Cr (59) (SmI_a^*) 84 (67) SmC_a^* 119.5 (118.5) SmC_γ^* 120.5 (119.7) SmC_β^* 121.9 (121.2) SmC_α^* 123.0 (122.5) SmA^* 150.2 (149.5) I

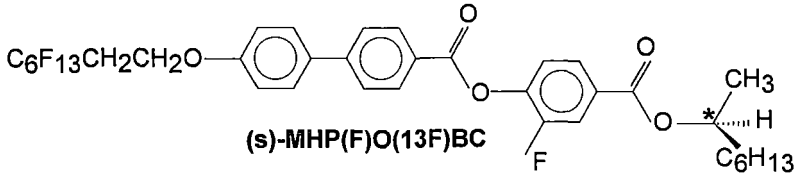

(s)-MHP(F)O(13F)BC

Cr 89.7 SmC^* 133.0 SmC_α^* 134.8 SmA^* 154.7 I

Figure 6.1. Molecular structure and phase behaviour of **(s)MHPO(13F)BC** and related compounds. Temperatures are in ^{0}C. Data of (s)MHPOBC are taken from [6] where data within parentheses refer to cooling cycle. Data of (s)MHP(F)O(13F)BC are taken from [13] where data within parentheses refer to cooling cycle.

crystal (AFLC) MHPOBC concluded that three *sub-phases* (SmC_α^* SmC_β^* and SmC_γ^*) could appear only in the AFLCs but they also suggested that SmC_α^* phase should be discussed separately. However, the present compound though shows no anticlinic order in the phase sequence, some indication of the presence of SmC_α^* *subphase* is observed. Existence of this phase was reported earlier in two pure non-AFLCs viz. 11HFBBBM7 and MHP(F)O(13F)BC by polarization hysteresis [12] and dielectric studies[13] respectively. It may be of interest to mention that though the former compound has quite different molecular structure, the second compound differs from the present one only by the presence of a fluorine group in the carbonyl-phenyl moiety (**Figure 6.1**). Other than studying the dielectric relaxation behaviour of the compound we were interested to see if the present compound also exhibited similar phase sequence.

Experimental

The molecular structure and phase transitions of S-(+)-4-(1-methylheptyloxy-carbonyl)phenyl 4'-(1H,1H, 2H, 2H perfluoroctyloxy)biphenyl-4-carboxylate [**MHPO(13F)BC**] are shown in **Figure 6.1**. Initial phase assignments and transition points were determined by monitoring the sample textures under a polarizing microscope, Mettler FP800 controller with FP82 hot stage was used as temperature controller. Setaram 141 differential scanning calorimeter was used to study the thermal behaviour and to determine the transition enthalpies.

ITO coated cells (EHC, Japan) of thickness 10 μm and effective area 4 mm^2 were used for complex dielectric permittivity measurements with HP 4192A impedance analyzer. Cell temperature was controlled by a Eurotherm temperature controller. Automatic data acquisition arrangement was made using a PC and RS232 interfacing. Measurements were made in SmA^* and SmC^* phases at 0.25^0C interval and at each temperature at 240 points in the frequency range 5 Hz to 13 MHz. The material was introduced into the cell in isotropic phase by capillary

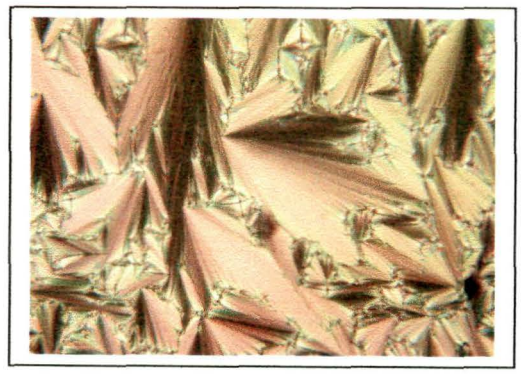

(a)

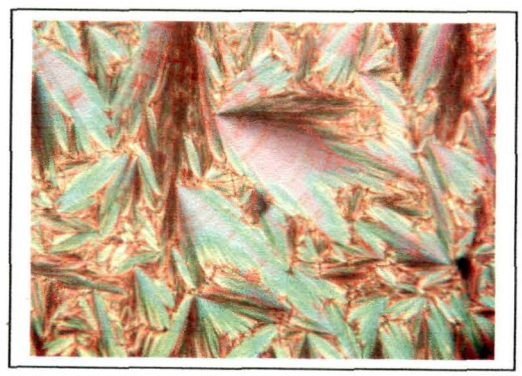

(b)

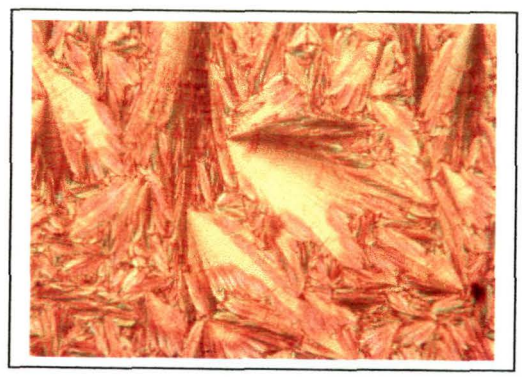

(c)

Figure 6.2. Textures observed under crossed polarizers (a) SmA^* phase at 157.7 ^{0}C, (b) SmC_α^* phase at 148.1 ^{0}C and (c) SmC^* phase at 140.0^{0}C.

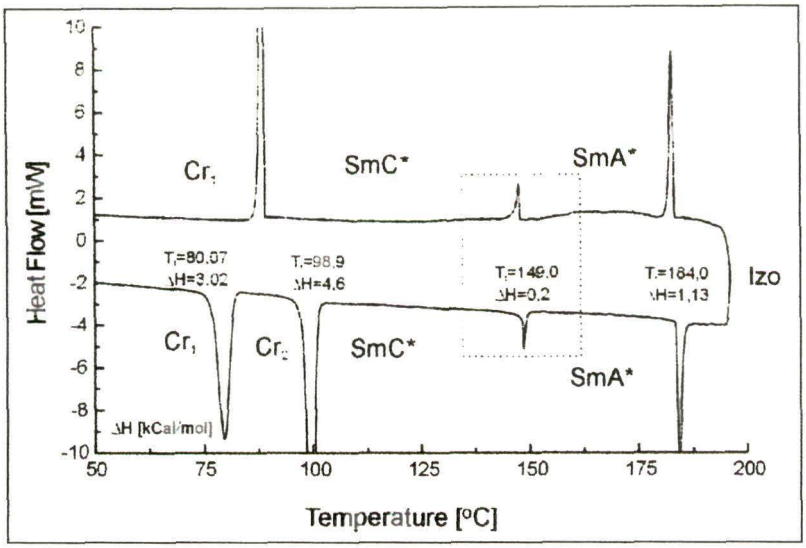

Figure 6.3. DSC traces obtained during heating and cooling, scan rate 2 K min^{-1}.

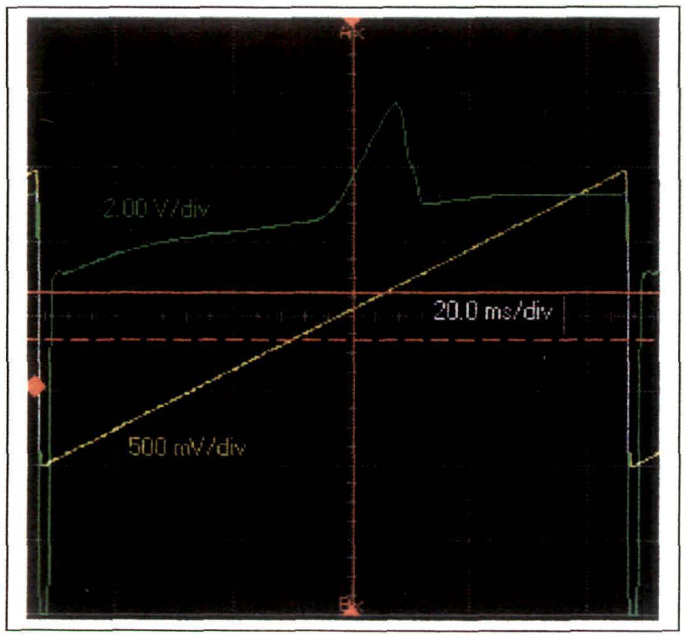

Figure 6.4. Image of the input and output signal captured in a digital oscilloscope during P_S measurement.

action and cooled it down very slowly. An electric field of 30 V_{pp} at 20Hz frequency was applied to obtain planar alignment. The quality of alignment was checked by polarizing microscopy and also by watching the time evolution of dielectric anisotropy.

Spontaneous polarization was measured as a function of temperature by reversal current method [14,15] using a triangular wave at 10 Hz obtained from HP 34401A function generator. The amplitude of the applied voltage was 20 V_{pp}. HP 500 MHz Infinium oscilloscope was used to record the voltage drop across a resistor as a function of time. Area under the curve was determined from the stored image after creating appropriate base line using a software developed for this purpose. P_S value was calculated using the expression $P_S = \int Vdt / (2AR)$ where A is the area of the cell, R is the resistance used to record the V-t curve.

Results and Discussions

Observed clearing point of **MHPO(13F)BC** is much higher than MHPOBC and unlike MHPOBC it does not exhibit anticlinic SmC_A^* phase as was also observed in MHP(F)O(13F)BC [13]. Textures revealed in optical polarizing microscopy are shown in **Figure 6.2**. Typical broken fan texture was observed in SmA^* phase. Clear evidence of the helix unwinding lines was observed in SmC^* phase. Within a small temperature range a subtle change is observed in the texture from those of the paraelectric SmA^* phase and the synclinic SmC^* phase, but the change in birefringence colour is distinct. However, the process is slow making it difficult to identify the exact transition point. DSC measurements, both during heating and cooling, also cannot detect any phase change in between SmA^* and SmC^*. DSC trace has been depicted in **Figure 6.3**. On the other hand, dielectric studies, as described below, show some anomalous thermal behaviour of P_S and the dielectric strength ($\Delta\varepsilon$) in between SmA^* and SmC^* phases in the narrow temperature range of 4.1 ^{0}C. This may be due to the presence of SmC_α^* phase.

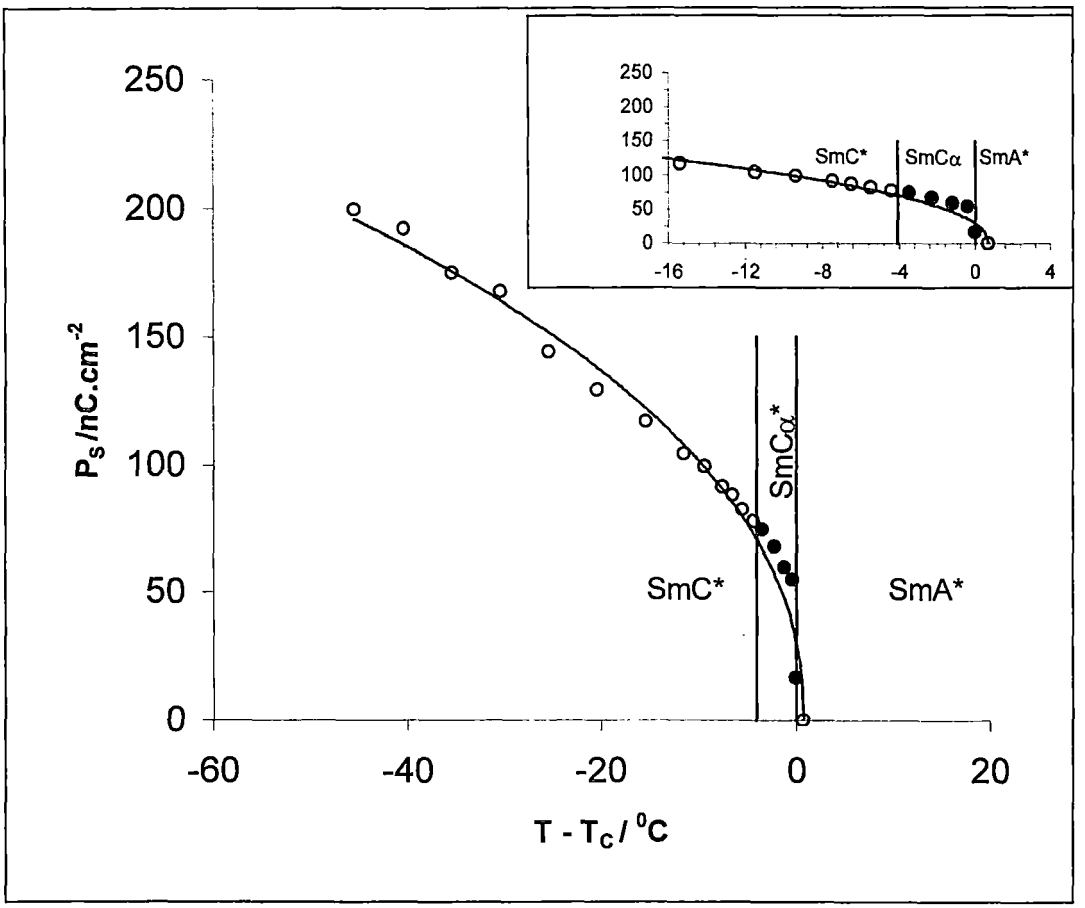

Figure 6.5. Variation of spontaneous polarization with temperature. Solid line represents fitted curve. Magnified view near T_C is shown in the inset. See text for details.

Dielectric study also reveals that the onset of SmA^* takes place at 145.5^0C which is 3.5^0C less than that observed by texture study. Moreover, when bias voltage (4 V_{pp}, 1 Hz) is applied in the cell, switching effect was observed under polarizing microscope from 145.5^0C till 91.5^0C though the compound showed crystalline phase up to at 98.9^0C during heating. Therefore, combining the optical microscopy, DSC and dielectric results the following phase sequence is proposed for **MHPO(13F)BC** during cooling.

$$Cr1\ 91.5\ SmC^*\ 141.4\ SmC_\alpha^*\ 145.5\ SmA^*\ 180.8\ I$$

Spontaneous polarization (P_S) was determined by reversal current method. Exemplary response voltage peaks obtained during electro-optic measurements is shown in **Figure 6.4**. This was obtained at 142.0^0C on the application of a triangular wave field of amplitude 20 V_{pp} at 10 Hz. Two peaks were observed at 5 Hz frequency and 4 peaks at 1 Hz frequency. Similarly, at 10 Hz frequency but with amplitude of 40 V_{pp} two peaks were observed. All the measurements were, however, made at 20 V_{pp} and 10 Hz field where only one peak was observed. Temperature dependence of the spontaneous polarization (P_S), calculated from the peak area, is shown in **Figure 6.5**. Rutkowska *et al.* [16] observed maximum value of P_S about 120 $nCcm^{-2}$ in SmC^* of MHPOBC which means that the fluorinated compound has much higher value (~200 $nCcm^{-2}$). Though while comparing P_S values one should keep in mind that it depends on the thickness of the cell and also on the nature of alignment within the cell. Similar results have been reported earlier in other fluorinated compounds [17,18]. According to the mean field model P_S should obey the relation $P_S = P_0 (T_C - T)^\beta$ where Tc is the paraelectric-ferroelectric (SmA^* - SmC^*) transition temperature [19,20]. For a second order transition β should be equal to 0.5. Measured data fit nicely to the above equation by least squares method, as shown in **Figure 6.5**, for parameter values $P_0 = 35.05 \pm 1.88$, $T_C = 146.20 \pm 0.01$ and $\beta = 0.45 \pm 0.02$. Thus the nature of the observed

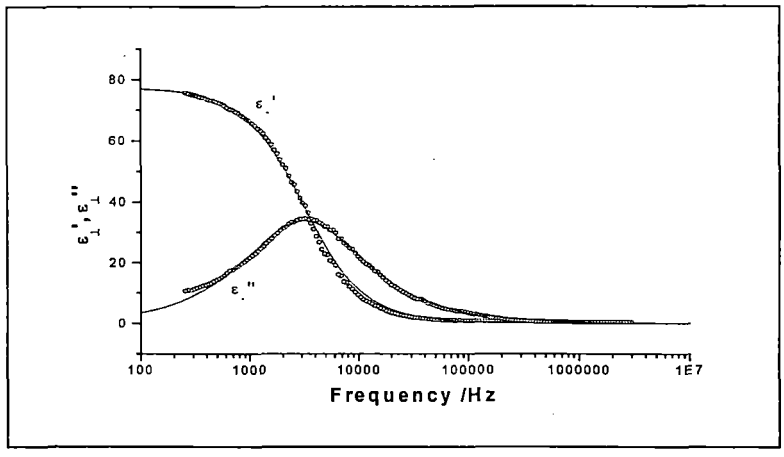

Figure 6.6: Dielectric spectra at 137.9^{0}C in SmC* phase. Curve fitted to Cole-Cole function is also shown as soild line.

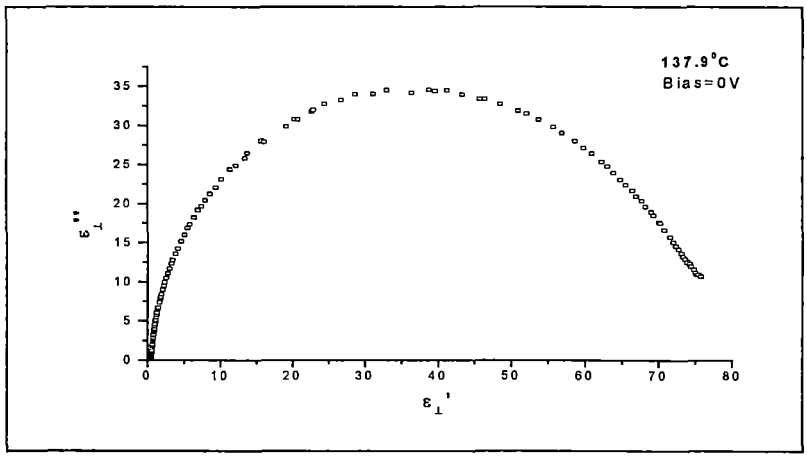

Figure 6.7. Cole-Cole Plot at 137.9^{0}C in SmC* phase.

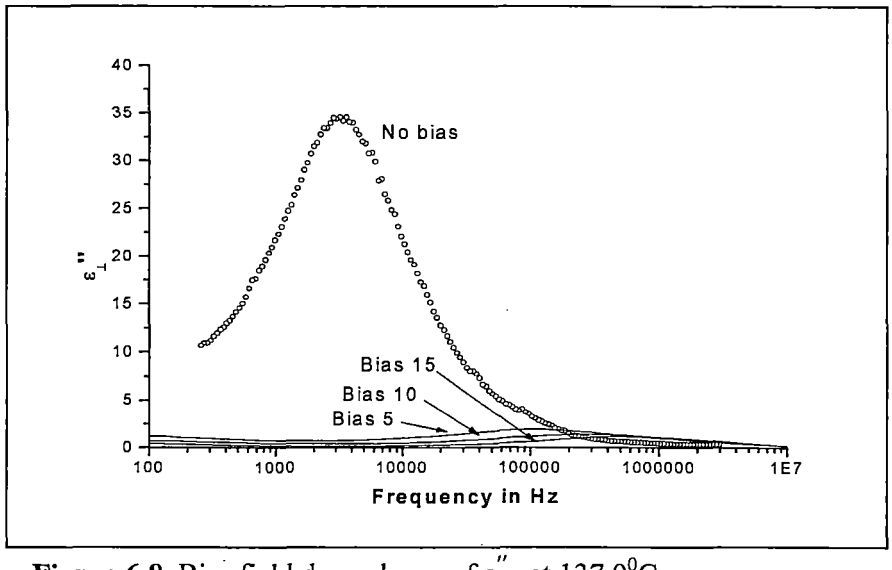

Figure 6.8. Bias field dependence of $\varepsilon''_{\perp}$ at 137.9^{0}C.

transition is not strictly second order. According to Clark and Lagerwall [21] in majority of the reported cases SmC^* phase is formed by cooling from the SmA^* phase through a second order phase transition. But when SmC^* phase is created directly from the nematic or from the isotropic liquid phase, layers of tilted molecules have to appear directly at the transition which makes the transition first order. However, in the case of fluorinated compounds SmA - SmC^* transitions have been found to be first order [22]. Enthalpy value of 0.2 kCal/mol at this transition in the present compound is indicative of first order phase transition.

A closer look in **Figure 6.5** also reveals a small but clear anomaly in the P_S values within the temperature range of 141.4 and 145.5^{0}C with respect to the fitted values (inset of **Figure 6.5**). This, it is presumed, gives another signal of the presence of SmC_α^* phase. No such anomaly is observed for direct transition to SmA^* from SmC^* phase [18, 23].

In **Figure 6.6** the real and imaginary components of the complex dielectric permittivity is shown as a function of frequency of the applied ac field at temperature 137.9^{0}C well within SmC^* phase. The exemplary spectra show typical dispersion behavior in $\varepsilon'_\perp$ and absorption behavior in $\varepsilon''_\perp$. Dependence of the two permittivities in the form of Cole-Cole plot is shown in **Figure 6.7**. The dielectric spectrum shows one distinct absorption peak that is related with the Goldstone mode (GM) relaxation behavior. Since in the Goldstone mode the dielectric increment ($\Delta\varepsilon=\varepsilon'_\infty - \varepsilon'_0$) is large (~79) it is difficult to study the soft mode (SM) properties in the SmC^* phase. This problem can, however, be overcome by applying a dc electric field, called bias field, in addition to the ac field. If this bias field is strong enough to unwind the helicoidal structure of the polarization vector then the Goldstone mode is completely suppressed and soft mode relaxation behavior appears in the spectrum [24,25]. In **Figure 6.8** the bias field dependence of $\varepsilon''_\perp$ is shown. It is clear that in **MHPO(13F)BC** a bias field of 15V is sufficient to suppress the Goldstone mode. Appearance of the Soft mode in SmC^* phase is

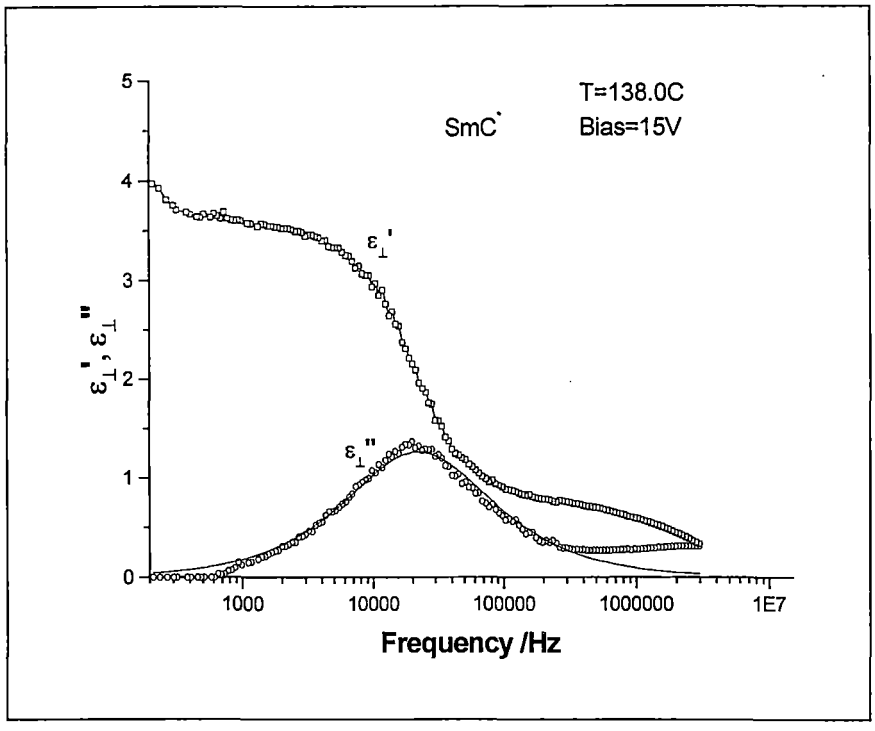

Figure 6.9: Dielectric spectra at 138.0^{0}C in SmC* phase with bias voltage. Curve fitted to Cole-Cole function is also shown as solid line.

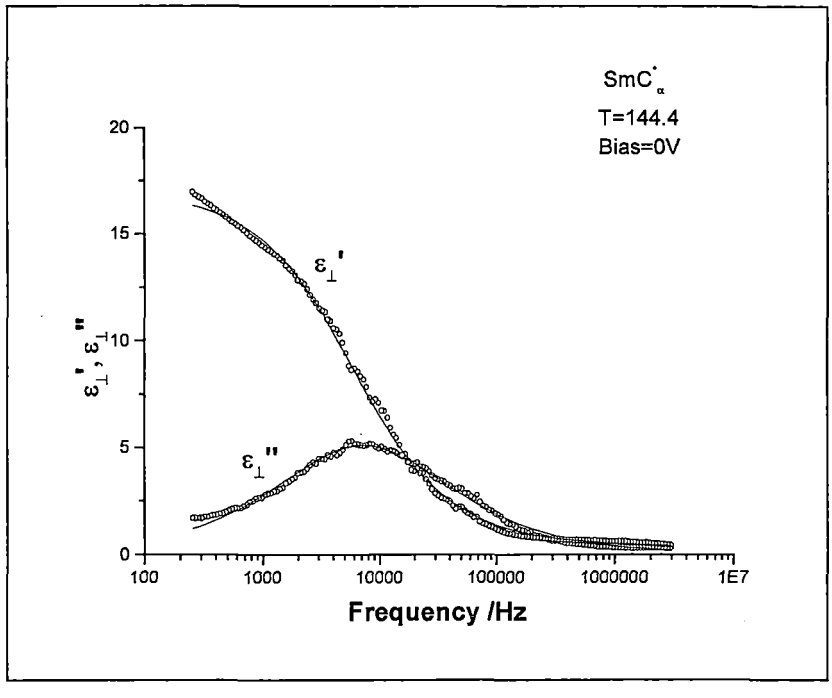

Figure 6.10. Dielectric spectra at 144.4^{0}C in SmC$_\alpha^*$ phase. Curve fitted to Cole-Cole function is also shown as solid line.

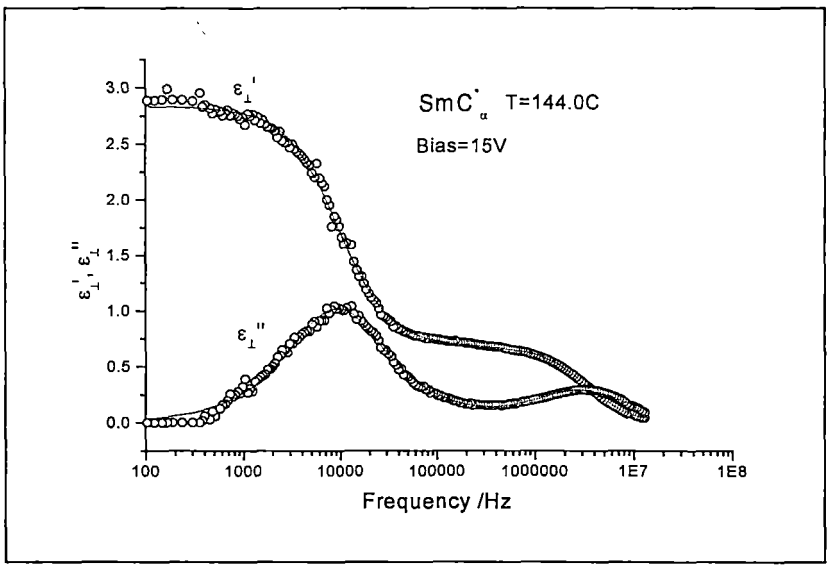

Figure 6.11. Dielectric spectra at 144.0^{0}C in SmC_α^* phase with bias. Curve fitted to Cole-Cole function is also shown as solid line.

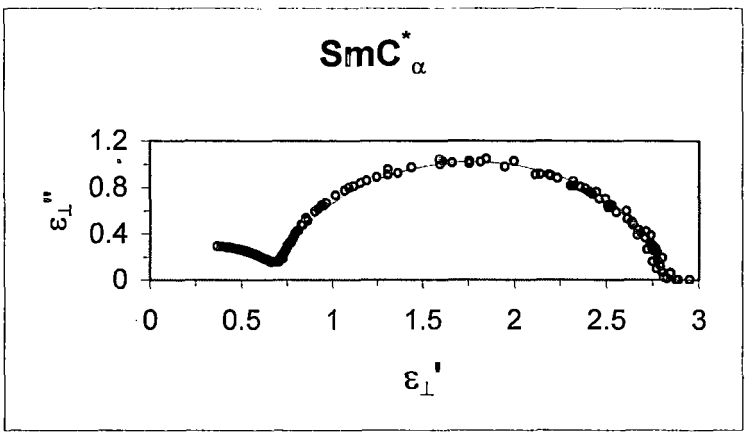

Figure 6.12. Cole-Cole plot at 144.0^{0}C with bias voltage in SmC_α^* phase.

Table 6.1. Values of the critical frequency (f_c), dielectric strength ($\Delta\varepsilon$) and dispersion parameter (α) in different phases.

Phase	Temperature (^{0}C)	Mode	Dielectric Strength	Critical frequency (kHz)	Dispersion parameter
SmC*	137.9	GM	79.2 ± 0.3	3.09 ± 0.02	0.10 ± 0.01
	138.0	SM	2.99 ± 0.05	22.1 ± 0.6	0.11 ± 0.01
SmC_α^*	144.4	GM	15.95 ± 0.09	7.22 ± 0.08	0.28 ± 0.01
	144.0	SM	2.82 ± .02	9.89 ± 0.01	0.06 ± 0.005
SmA*	145.9	SM	3.11 ± 0.04	55.60 ± 1.34	0.13 ± 0.01

evident from the bias-dependent spectra (**Figure 6.9**). The spectra (**Figures 6.6 and 6.9**) were fitted by non-linear least squares method to the Cole-Cole function [26], described in Chapter II, using the software Origin. Obtained fitted parameters are: dielectric increment $\Delta\varepsilon$=79.2 ± 0.3, critical frequency f_c=3.09 ± 0.02 kHz (GM), dispersion parameter α=0.10 ± 0.01 without bias at 137.9^{0}C and $\Delta\varepsilon$=2.99 ± 0.05, f_c=22.1 ± 0.6 kHz (SM) and α=0.11 ± 0.01 with bias in SmC* phase at 138.0^{0}C.

In SmC$_\alpha^*$ phase the observed frequency domain spectra at 144.4^{0}C is shown in **Figure 6.10** depicting the GM mode. Dielectric strength is reduced to 20% of the value in SmC* phase whereas the critical frequency is increased by a factor 2.3. The observed values can be fitted to the Cole-Cole function with parameter values: $\Delta\varepsilon$=15.95 ± 0.09, f_c=7.22 ± 0.08 kHz, α=0.28 ± 0.01 when no bias field is applied. The spectra obtained at 144.0^{0}C with a dc bias of 15V are shown in **Figure 6.11.** Corresponding Cole-Cole plot is shown in **Figure 6.12.** In this case two absorption peaks are observed. The peak in MHz region is actually an ITO peak which was confirmed by taking spectra of an empty cell, the peak in kHz region is the SM peak. We, therefore, fitted the spectra to the Cole-Cole function but with another term for the second peak. Fitted parameters are $\Delta\varepsilon_{SM}$ = 2.82 ± .02, f_{cSM} = 9.89 ± 0.01 kHz, α_{SM} = 0.06 ± 0.005, $\Delta\varepsilon_{ITO}$ = 0.58 ± .02, f_{cITO} = 3.33 ± 0.2 MHz, α_{ITO} = 0.02 ± 0.005.

Typical absorption and dispersion spectra are observed in SmA* phase and as expected no change in spectra is observed when bias field is applied. The critical frequency of the soft mode is found to be much higher than that in SmC* or in SmC$_\alpha^*$phase. However, the dielectric increment and the dispersion parameter values do not change much. The spectra at 145.9^{0}C was fitted to the Cole-Cole function with parameter values, $\Delta\varepsilon$=3.11 ± 0.04, f_c=55.60 ± 1.34 kHz, α=0.13 ± 0.01. Values of the critical frequency (f_c), dielectric strength ($\Delta\varepsilon$) and dispersion parameter (α) are collected in **Table 6.1** for easy comparison.

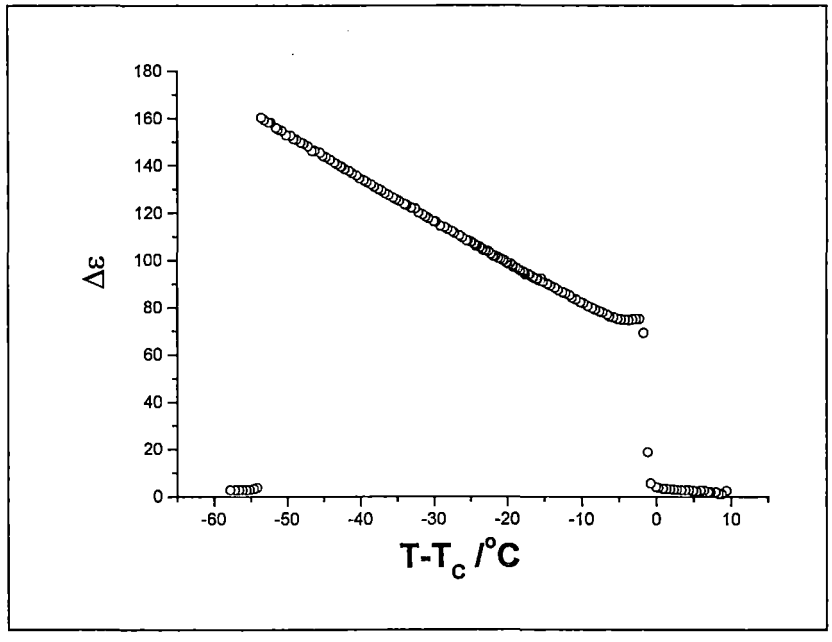

Figure 6.13. Variation of dielectric strength with temperature.

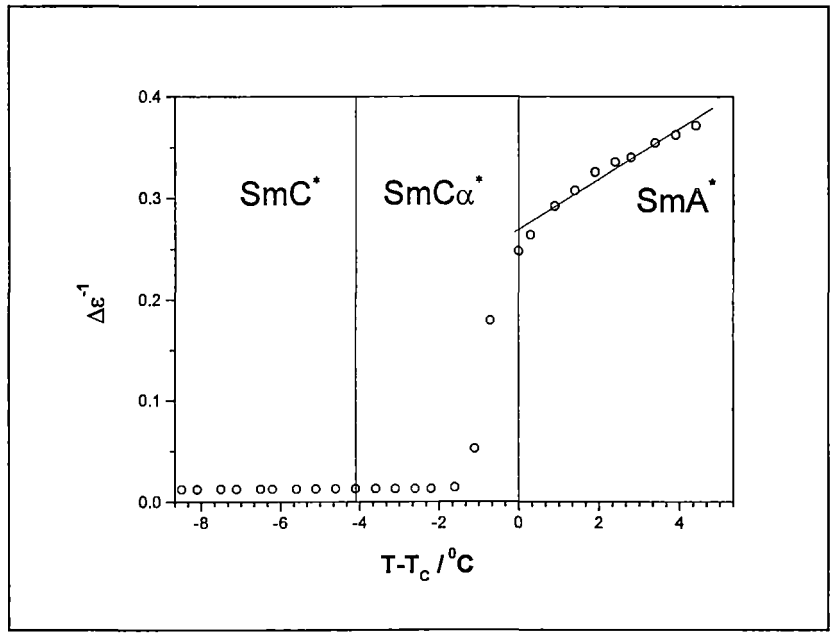

Figure 6.14. Temperature variation of inverse dielectric strength in the vicinity of T_C. Slope of the fitted line is 0.025 ± 0.002 and intercept 0.269 ± 0.005.

The temperature dependence of the dielectric strength ($\Delta\varepsilon$) is shown in **Figure 6.13** when no bias field is applied. Three anomalies are seen in the graph. One at the Cr-SmC* transition, next one at SmC* - SmC$_\alpha^*$ transition and the third one at the SmC$_\alpha^*$ - SmA* transition. Variation of the reciprocal dielectric strength ($\Delta\varepsilon^{-1}$) near SmC$_\alpha^*$ phase is shown in **Figure 6.14** from which it is very clear that the rate of change of $\Delta\varepsilon^{-1}$ at SmC* - SmC$_\alpha^*$ and at SmC$_\alpha^*$ - SmA* is different. In para-electric phase though $\Delta\varepsilon^{-1}$ increases with T and show the Curie-Weiss behavior as expected from Landau theory.

Thus the compound **MHPO(13F)BC** may also possess SmC$_\alpha^*$ phase between the ferroelectric SmC* and paraelectric SmA* phase as was observed in the related compound **MHP(F)O(13F)BC** [13]. Moreover, the stability of SmC$_\alpha^*$ phase is more (4.1^0C) in this case than the previous compound (1.8^0C). The structure of SmC$_\alpha^*$ phase is rather complex and not yet well understood. Different models have been proposed to explain the observed behaviour. This phase was described as a tilted ferroelectric like phase in its low temperature range, as an antiferroelectric phase in the high temperature range and as ferrielectric-like in the intermediate range. So a structural model bearing features of a devil's staircase was proposed [27-30]. M. Cepic and B. Žekš [31] proposed a discrete model for the phase. It was also shown that the SmC$_\alpha^*$ *sub phase* is ferroelectric-like with a very short pitch of the helix and the phase angle difference between the directors in neighbouring layers can be between 0 and π [13,32,33]. Recent X-ray results indicate an incommensurate periodicity, evolving from 5 to 8 smectic layers with increasing temperature, in this phase [34]. The values of $\Delta\varepsilon$ in SmC$_\alpha^*$ phase of the present compound also suggest that in the low T range its behaviour is ferroelectric type and in the high T region it is antiferroelectric type though ferrielectric behaviour is observed in the mid T range [28,29]. The compounds 11HFBBBM7 and MHP(F)O(13F)BC also exhibited similar to kind of behaviour.

References

1. R. B. Meyer, Paper presented at the 5^{th} *Int. Liquid Crystal Conf.*, Stockholm, June, (1974).
2. R. B. Meyer, L. Liebert, L. Strzelecki and P. Kelkar, *J Phys (Paris) Lett.* **36**:L69 (1975).
3. A. D. L. Chandani, Y. Ouchi, H. Takezoe, A. Fakuda, K. Terashima, K. Furukawa and A. Kishi, *Jpn. J. Appl. Phys.* Part 2, **28**, L1261 (1989).
4. Y. Izozaki, T. Fujikawa, H. Takezoe, A. Fukuda, T. Hagiwara, Y. Suzuki and I. Kawamura, *Phys. Rev. B*, **48**,13439 (1993).
5. J. P. F. Lagerwall, D. D. Parghi, D. Kruerke, F. Gouda, and P. Jagemalm, *Liq.Cryst.*, **29**, 163 (2002).
6. J. P. F. Lagerwall, P. Rudquist, and S.T. Lagerwall, *Liq. Cryst.*, **30**, 399 (2003).
7. E. Gorecka, D. Pociecha, M. Čepič, B. Žekš, R. Dabrowski, , *Phys. Rev. E* **65**, 061703 (2002).
8. K. Miyachi and A. Fukuda, In *Handbook of Liquid Crystals*, Eds. D. Demus, J. Goodby, G. W. Gray, H. W. Spiess and V. Vill, Wiley-VCH, Vol. **2B**, p.665, (1998).
9. S. T. Lagerwall, A. Dahlgren, P. Jagemalm, P. Rudquist, K. DHavé, H., Pauwels, R. Dabrowski and W. Drzewinski, *Adv. Funct. Mater.*, **11**, 87 (2001).
10. I. Dierking, *J. Phys.*: *Condens. Matter*, **16**, 1715 (2004).
11. A. M. Biradar, S. Wróbel, and W. Haase, *Phys. Rev. A*, **39**, 2693 (1989).
12. S. Sarmento, P. S. Carvalho, M. R. Chaves, H. T. Nguyen, and F., Pinto, *Mol.Cryst. Liq. Cryst.*, **328**, 457 (1999).
13. M. Marzec, A. Mikulko, S. Wróbel, R. Dabrowski, M. Darius and W. Haase, *Liq. Cryst.*, **31**,153 (2004).
14. K. Miyasato, S. Abe, H. Takezoe, A. Fukuda and E. Kuze, Jpn. J. Appl. Phys., **22**, L661 (1983); A. Fukuda, Y. Takanishi, T. Izozaki, K. Ishikawa and H. Takezoe, *J. Mater. Chem.* **4**, 997 (1994).
15. J. Hou, J. Schacht, F. Gießelmann and P. Zugenmaier, *Liq. Cryst.*, **22**, 401 (1997).
16. J. Rutkowska, P. Perkowski, J. Kedzierski, Z. Raszewski, R. Dabrowski, S. Gauza, and K. Czuprynski, , *Mol. Cryst. Liq. Cryst.*, **366**, 617 (2001).
17. J. W. Goodby, In *Ferroelectric Liquid Crystals Principles, Properties and Applications*, J. W. Goodby, R. Blinc, N.A. Clark, S.T. Lagerwall, M.A. Osipov, S.A. Pikin, T. Sakurai, K. Yoshino, and B. Žekš, Gordon and Breach Science Publishers, Philadelphia, p191 (1991).
18. M. Marzec, J. Popczyk, A. Farara, S. Wróbel and R. Dabrowski, *Ferroelectrics*, **281**, 123 (2002).
19. F. Gouda, T. Carlsson, G. Andersson, S.T. Lagerwall, and B. Stebler, *Liq. Cryst.*, **2**, 315 (1994).
20. T. Carlsson, B. Žekš, and R. Blinc, *Phys. Rev.*, A**38**, 5833 (1988).
21. N. A. Clark and S. T. Lagerwall, in *Ferroelectric Liquid Crystals Principles, Properties and Applications*, J. W. Goodby, R. Blinc, N.A. Clark, S.T. Lagerwall, M.A. Osipov, S.A. Pikin, T. Sakurai, K. Yoshino, and B. Žekš (Eds.), Gordon and Breach Science Publishers, Philadelphia, p3 (1991).
22. R. Dabrowski, J. Gasowska, J. Otón, W. Piecek, J. Przedmojski, M. Tykarska, *Displays*, **25**, 9 (2004).
23. Z. Raszewski, J. Kedzierski, J. Rutkowska, W. Piecek, P. Perkowski, K. Czuprynski, R. Dabrowski, W. Drzewinski, J. Zielinski, and J. Zmija, *Mol.Cryst. Liq. Cryst.*, **366**, 607 (2001).
24. J. Pavel and M. Glogarova, *Ferroelectrics*, **84**, 241 (1989).

25. F. Gouda, G. Andersson, T. Carlsson, S.T. Lagerwall, K. Sharp, B. Stebler, C. Filipic, B. Žekš, and A. Levstik, *Mol. Cryst. Liq. Cryst. Lett.*, **6**, 151 (1989).
26. S. Wróbel in *Relaxation phenomena* – Liquid crystals, magnetic systems, polymers, high-T_C superconductors, metallic glasses, Haase W., and Wróbel, S., (Eds), Springer-Verlag, Berlin-Heidelberg, p20 (2003).
27. Y. Takanishi, K. Hiraoka, V. Agarwal, H. Takezoe, A. Fukuda and M. Matsushita, *Jpn. J. Appl. Phys.*, **30**, 2023 (1991).
28. C. Bahr, D. Fliegner, C. J. Booth, and J. W.Goodby, *Phys. Rev.*E, **51**, R3823 (1995).
29. V. Laux, N. Isaert, G. Joly and H. T. Nguyen, *Liq. Cryst.*, **26**, 361 (1999).
30. P. Bak, Phys. Today, **39**(12), 38, 1986.
31. M. Cepic and B. Žekš, *Mol. Cryst. Liq. Cryst.*, **263**, 61 (1995).
32. J. Ortega, C. L. Folcia, J. Etxebarnia and M. B. Ros, *Liq. Cryst.*, **30**, 109 (2003).
33. M. Skarabot, M. Cepic, B. Zeks, R. Blinc, G. Heppke, A.V. Kityk and I. Musevic, *Phys. Rev.*E, **58**, 575 (1998).
34. P. Mach, R. Pindak, A. -M. Levelut, P. Barios, H. T. Nguyen, C. C. Huang, and L. Furenlid, *Phys. Rev. Lett.*, **81**, 1015 (1998).